Detecting a preformed pair phase: Response to a pairing forcing field

A. Tagliavini,[1] M. Capone,[2] and A. Toschi[1]
[1]*Institute for Solid State Physics, Vienna University of Technology, 1040 Vienna, Austria*
[2]*International School for Advanced Studies (SISSA), Via Bonomea 265, I-34136 Trieste, Italy*
(Received 9 May 2016; revised manuscript received 9 September 2016; published 10 October 2016)

The normal state of strongly coupled superconductors is characterized by the presence of "preformed" Cooper pairs well above the superconducting critical temperature. In this regime, the electrons are paired, but they lack the phase coherence necessary for superconductivity. The existence of preformed pairs implies the existence of a characteristic energy scale associated with a pseudogap. Preformed pairs are often invoked to interpret systems where some signatures of pairing are present without actual superconductivity, but an unambiguous theoretical characterization of a preformed-pair system is still lacking. To fill this gap, we consider the response to an external pairing field of an attractive Hubbard model, which hosts one of the cleanest realizations of a preformed pair phase, and a repulsive model where *s*-wave superconductivity cannot be realized. Using dynamical mean-field theory to study this response, we identify the characteristic features which distinguish the reaction of a preformed pair state from a normal metal without any precursor of pairing. The theoretical detection of preformed pairs is associated with the behavior of the *second* derivative of the order parameter with respect to the external field, as confirmed by analytic calculations in limiting cases. Our findings provide a solid test bed for the interpretation of state-of-the-art calculations for the normal state of the doped Hubbard model in terms of *d*-wave preformed pairs and, in perspective, of nonequilibrium experiments in high-temperature superconductors.

DOI: 10.1103/PhysRevB.94.155114

I. INTRODUCTION

In many complex materials and quantum systems we witness the persistence of fingerprints of superconductivity well above the critical temperature and clearly distinct from fluctuation phenomena. This often leads to a possible interpretation in terms of electron pairs which are formed at very large temperature but they can condense only at a much lower critical temperature due to the phase fluctuations of their wave function. Yet, the unambiguous detection of preformed pairs is elusive, as it does not correspond to an actual phase transition and it cannot be unambiguously associated with a direct observable quantity.

The prototypical realization of this physics takes place in model systems with strong pairing interaction, which drives the formation of tightly bound pairs with a reduced phase coherence. In this regime, superconductivity occurs as a Bose-Einstein condensation (BEC) of composite bosons formed by the bound pairs of fermions. When the pairing strength is tuned from weak to strong coupling one observes a continuous crossover from the familiar BCS [1] pairing to this regime.

This BCS-BEC crossover [2–6] has been intensively studied, both in the context of cold atoms trapped in optical lattices [7] and in high-temperature superconductivity, where a preformed pair regime has been invoked [8–12] for the pseudogap state [13,14] of underdoped cuprates.

In this work we use the attractive Hubbard model as a theoretical device to set a *practical protocol* to confirm or disprove the existence of preformed pairs in a specific system under analysis. Comparing regimes where *s*-wave preformed pairs are certainly present or certainly absent, we identify which properties of the system are so sensitive to their presence to be exploited for their detection. Such an identification will also be applicable to interpret existing analyses of the pseudogap phase in the cuprates [15–17].

We have structured our paper as follows: In Sec. II, we briefly discuss the modelization of the problem, in terms of the single-band (attractive) Hubbard Hamiltonian, and briefly review some of the previous dynamical mean-field theory (DMFT) studies in the absence of an external field. In Sec. III, we report our DMFT results in the presence of a forcing field at different temperatures and interactions, comparing explicitly the attractive and repulsive models. The physical interpretation of our numerical results in terms of the underlying ground-state properties is given in Sec. IV. In Sec. V we discuss the implication of this criterion in a broader context, while in Sec. VI we present our conclusions.

II. MODELIZATION OF THE PROBLEM

Throughout this paper we will consider a simple Hubbard model in the presence of an external field driving an *s*-wave superconducting order parameter:

$$H = -t \sum_{\langle ij\rangle\sigma} c^{\dagger}_{i\sigma} c_{j\sigma} + U \sum_{i} n_{i\uparrow} n_{i\downarrow} - \mu \sum_{i\sigma} n_{i\sigma} - \eta \sum_{i} (c^{\dagger}_{i\uparrow} c^{\dagger}_{i\downarrow} + \text{H.c.}). \quad (1)$$

Here, t represents the nearest-neighbor amplitude, μ is the chemical potential, and the effective interaction U is negative for the *attractive* and positive for the *repulsive* Hubbard model. The last contribution in Eq. (1) represents the coupling of the system to a forcing, time-independent pairing field η, which is assumed to be positive and isotropic (*s* wave).

In more than two dimensions the attractive Hubbard model displays a low-temperature *s*-wave superconductivity, smoothly evolving from a weak-coupling (BCS) regime to a strong-coupling BEC regime with increasing U [18]. In the latter regime, pairs are formed at a very high temperature of order U, while they can only condense at a much lower temperature $T = T_c \propto \frac{1}{U}$ because of the large phase fluctuations which contrast the formation of a coherent condensate [2]. In the BCS regime, superconductivity is stabilized by a potential energy

gain, while the superconductor has a (slightly) higher kinetic energy than the normal state. In the BEC regime the energetic balance is the opposite: The superconductor is stabilized by a kinetic energy gain with a slight potential energy loss with respect to the normal state [18].

Given the s-wave nature of the pairs and the local nature of the interactions, much of the physics for $d > 2$ can be well captured by dynamical mean-field theory (DMFT) [19], an approach where spatial fluctuations are frozen, but the local dynamics is included nonperturbatively at every value of the interaction strength. DMFT becomes formally exact in the limit of infinite coordination [20] of the lattice but it can be used as an approximation in finite dimensions, where it provides a fully nonperturbative description. This represents a major advantage to analyze weak- and strong-coupling regimes on equal footing. Previous DMFT studies [18,21–23] have focused on spectral, thermodynamic properties, and even on some nonequilibrium properties [24]. Here we consider a different aspect, namely the response to an external stimulus which drives a superconducting s-wave pairing, also beyond the linear-response regime.

For the sake of definiteness we consider a semicircular density of states $N(\epsilon) = \frac{2}{\pi D^2}\sqrt{D^2 - \epsilon^2}$ (D being its half-bandwidth) which is suitable to represent a finite-bandwidth system in DMFT. To solve the auxiliary impurity problem of DMFT we adopted an exact diagonalization (ED) solver with $n_s = 5$ sites (one impurity and $n_b = 4$ bath electronic sites), and tested the stability of the results by increasing the number of sites in the most relevant intermediate-coupling/low-temperature regime. Obviously, due to the external pairing field in Eq. (1), the DMFT treatment has to be extended to the broken-symmetry phase, by recasting DMFT in Nambu formalism (see, e.g., [22]).

In this section we set up the stage by presenting refined results for the unperturbed attractive Hubbard model. In this way we identify concretely weak-, intermediate-, and strong-coupling regions whose definition will be helpful to guide the discussion of the following sections.

Figure 1 shows the energy difference between the superconducting and the normal state $\Delta E_{tot} = E_S - E_N$ (resolved in its kinetic and potential energy components) in different interaction regimes for two significant choices of the electron density: $n = 1$ (half filling) and $n = 0.5$ (quarter filling). We consider a low value of the temperature $\beta = 50D^{-1}$ which is significantly below T_c for the broad range of $|U|$ used in the figure. Moreover, we verified that discretization effects associated with a finite bath size of the ED solver are negligible.

Our findings are summarized by the different colors in the diagrams, which mark the different regimes (BCS: blue; intermediate: violet; BEC: red). Figure 1 shows that a qualitative change of the energetic balance with respect to BCS only takes place when $U \simeq 2D$, where a narrow intermediate region, in which the superconductor gains both potential and kinetic energy, starts. At $U \simeq 2.5D$ a BEC regime is established. This evolution of the energetic balance tracks the progressive formation of preformed pairs in the normal state. These results provide a more accurate determination of the boundaries found in Ref. [18]. We also notice that the results for $n = 1$ and $n = 0.5$ are remarkably similar. This observation shows how weakly the physics of the attractive

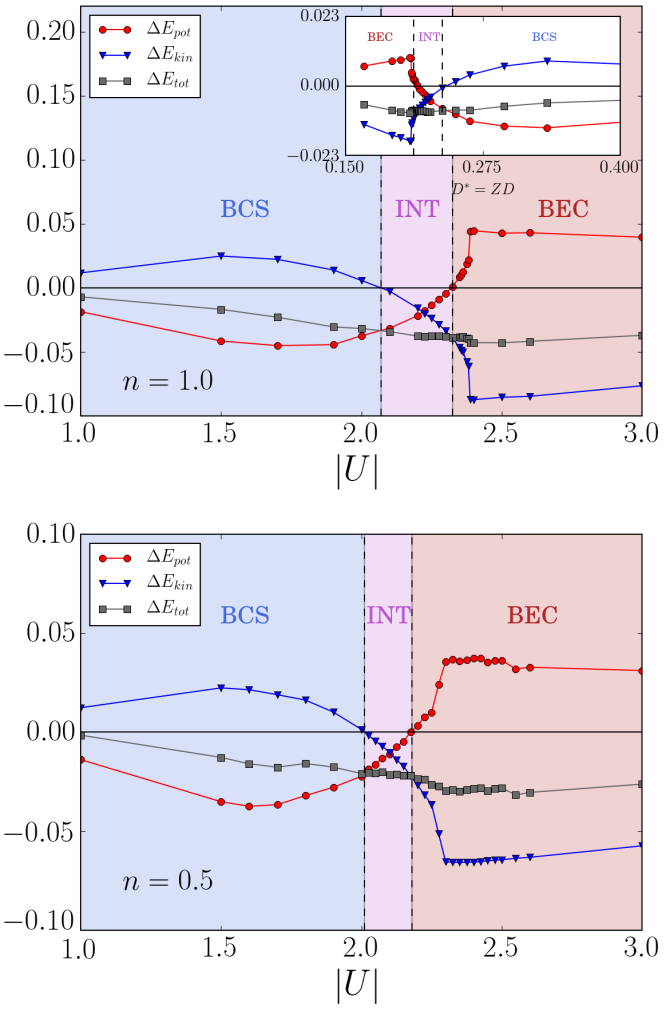

FIG. 1. Energy balance $\Delta E_{tot} = E_S - E_N$ (and its kinetic and potential components) computed in the superconducting region at $\beta = 50D^{-1}$ as a function of the attractive interaction U. The upper panel refers to the half-filled ($n = 1$) case, while the lower panel refers to the electron density $n = 0.5$. Inset: The same but for the Hamiltonian of Eq. (2), where the energies have been scaled in order to keep the attractive interaction constant ($\lambda = -0.5$) and let the bandwidth vary as a more realistic effect of the correlation and/or doping.

Hubbard model depends on doping. For this reason we will mainly focus in the following on the half-filled case, which has an important practical advantage for our calculations, which are performed in the grand-canonical ensemble, where the chemical potential is the independent variable. The half-filling condition is indeed obtained by enforcing particle-hole symmetry, which corresponds to $\mu = U/2$. For any other filling, the corresponding chemical potential and its dependence on U are not known analytically and they must be found numerically. We however show explicitly that our findings are general by performing a set of calculations for $n = 0.5$. Analogous DMFT characterizations also hold for magnetic phases, in particular for the "sibling" crossover from a Slater to an Heisenberg antiferromagnet, as explicitly shown by recent DMFT [25] and dynamical cluster approximation (DCA) [26] results.

In this work the attractive Hubbard is not introduced as a microscopic description of any realistic material, but as a simple tool for the detection of preformed pairs. However, the energetic analysis we just summarized was suggested as a possible explanation of the spectral weight changes observed in the optical conductivity on the cuprates [27–38]. Evidently any attempt in this direction must include at least qualitatively the effect of strong repulsive correlations, which mainly control the doping dependence of the cuprate phase diagram. Thus, if one wanted to use Eq. (1) with $U = -\lambda < 0$ for a rough investigation of these specific features in the cuprate physics, one should account for the doping dependence of the quasiparticle properties. This can be achieved by renormalizing the kinetic term by means of the quasiparticle weight Z, while leaving at first approximation the effective attractive interaction unchanged:

$$H = -Z\,t \sum_{\langle ij\rangle,\sigma} c^{\dagger}_{i\sigma} c_{j\sigma} - \lambda \sum_{i} n_{i\uparrow} n_{i\downarrow} - \mu \sum_{i} (n_{i\uparrow} + n_{i\downarrow}). \tag{2}$$

Here the effective bandwidth $D^* = 2Zt$ decreases as we reduce the hole doping and vanishes at the Mott transition $Z \to 0$ as $x \to 0$, while the attractive interaction λ is taken as a constant. Such a simple assumption is explicitly realized, e.g., in realistic modeling of the strongly correlated superconductivity in fullerides [39,40]. As for the energetic balance this amounts to a rescaling in the previous plot, whose effects are reported in the inset of Fig. 1: The results of this a "more physical" approach to the problem do not change the qualitative picture, making, however, the energetic balance between the BCS and the BEC regimes overall more symmetric.

III. DMFT RESULTS IN THE PRESENCE OF A FORCING FIELD

In this section we will apply a "theoretical probe" to investigate the preformed pair physics: We will study the superconducting response induced by a *finite* forcing pairing field, also *beyond* the linear response regime. We will compute by means of DMFT the s-wave superconducting order parameter $\Delta = \frac{1}{N}\sum_i \langle c_{i\downarrow} c_{i\uparrow}\rangle$ as a function of the external field η at different interaction couplings (U) and inverse temperatures ($\beta = 1/T$). We detail our analysis in the half-filling case, where particle-hole symmetry strongly reduces the time required by the calculations, and then we extend our investigation to a less symmetric case away from half filling, specifically for $n = 0.5$ (quarter filling).

A. Half-filling study ($n = 1.0$)

As a first step, we follow the evolution of $\Delta(\eta)$ in the attractive case ($U < 0$) across the critical temperature at weak- and strong-coupling regimes (according to the classification of Sec. II). This evolution shows the expected appearance of a finite Δ for $\eta = 0$ below T_c and the divergence of the slope of $\Delta(\eta)$ for $\eta \to 0^+$ (which coincides with the linear-response pairing susceptibility) approaching T_c from above (see Fig. 2).

These obvious features are a direct consequence of a second-order phase transition and could, thus, hide the

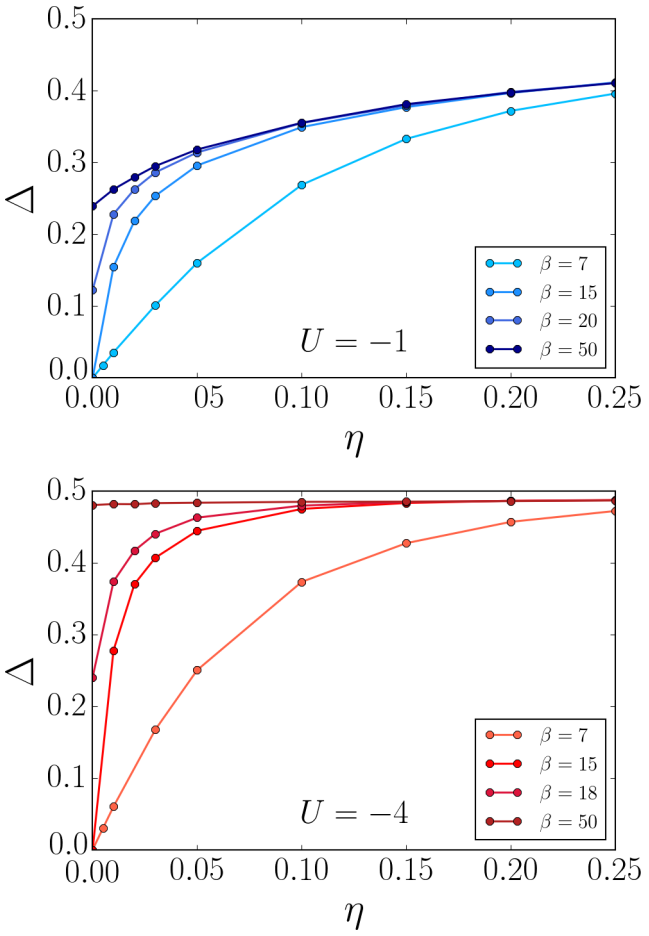

FIG. 2. Superconducting s-wave order parameter for two different values of the on-site attractive interaction, namely, $U = -1$ and $U = -4$, and for different β values at half filling.

preformed-pair physics. Hence, in the following analysis, we will choose a sufficiently high temperature $T = 1/7D$ (i.e., $T \gg T_c$ for the selected U) to be safely in the normal state and to mitigate the impact of the underlying phase transition on the low-η behavior of $\Delta(\eta)$.

The corresponding results are shown in Fig. 3 (left panel), where the exact result for the atomic limit ($t = 0$) is also reported for comparison. For all U values from weak to strong coupling and in the atomic limit $\Delta(\eta)$ saturates to 1/2 by increasing η. Physically, this reflects the fact that, due to the attractive interaction in the s-wave channel, the system responds promptly to the forcing pairing field: the slope of $\Delta(\eta)$ assumes the largest value for $\eta \to 0^+$ and decreases monotonically with η.

Mathematically, this means that $\Delta(\eta)$ is a *concave* function for the whole interval $\eta \in (0,\infty)$, i.e.,

$$\frac{d^2\Delta(\eta)}{d\eta^2} < 0 \quad \forall\, \eta > 0. \tag{3}$$

We note that this general property is totally unaffected by the specific behavior of the linear response regime (slope for $\eta \to 0^+$), whose quantitative change as a function of U mostly reflects a different proximity to T_c, which is maximum at intermediate coupling [18,41], very close to the reported

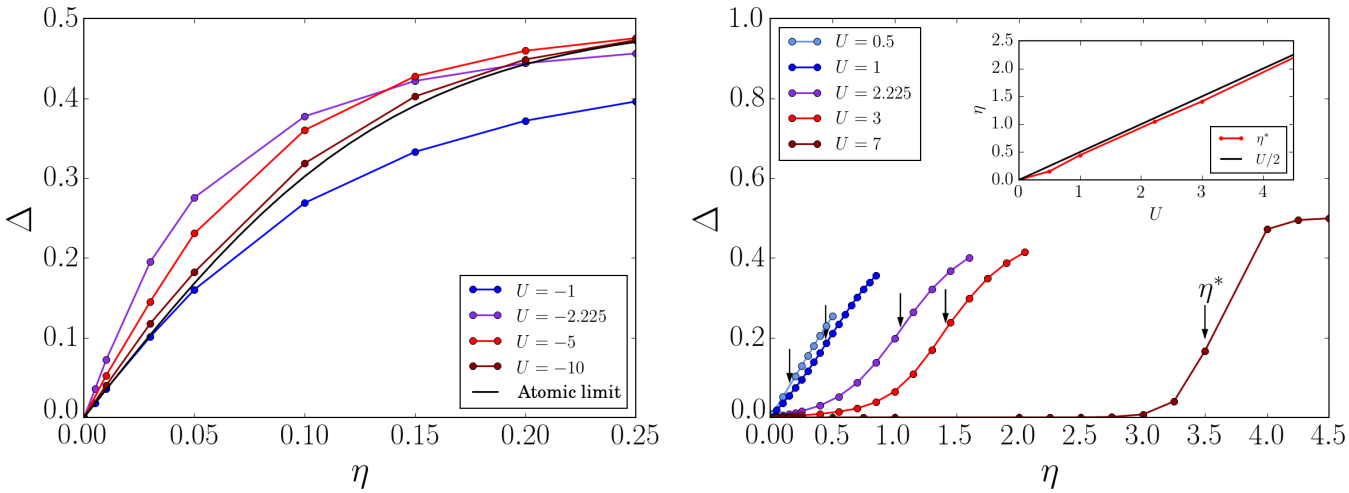

FIG. 3. Superconducting s-wave order parameter $\Delta = \frac{1}{N}\sum_i \langle c_{i\downarrow} c_{i\uparrow}\rangle$ as a function of the forcing pairing field η in the attractive (left panel) and the repulsive (right panel) Hubbard model (half-filling case). Here all the quantities are expressed in units of the half-bandwidth D. The black line on the right panel refers to the analytic behavior in the atomic limit at $\beta = 7$ [see Eq. (9)].

value of $U/D = -2.225$. This is exemplified in Fig. 4 where we perform the same analysis but for a *local* pairing field η_{loc} and detecting the local order parameter. Here the small-η slope, being proportional to the local pairing susceptibility, is unaffected by the proximity to the second-order phase transition, and it monotonically approaches the atomic limit result. Nevertheless, the curvature of the second-order derivative is the same as the one of the uniform-field case.

In order to understand the physical meaning of Eq. (3), and to exploit it for a preformed-pairs probing beyond our work, we provide a comparative DMFT study of the opposite situation, where our external pairing field η contrasts the underlying spontaneously ordered phase of the system at low T. This can be realized repeating the same analysis for the *repulsive* ($U > 0$) Hubbard model. The corresponding results are shown in Fig. 3 (right panel), where—as before—the s-wave superconducting order parameter is plotted as a function

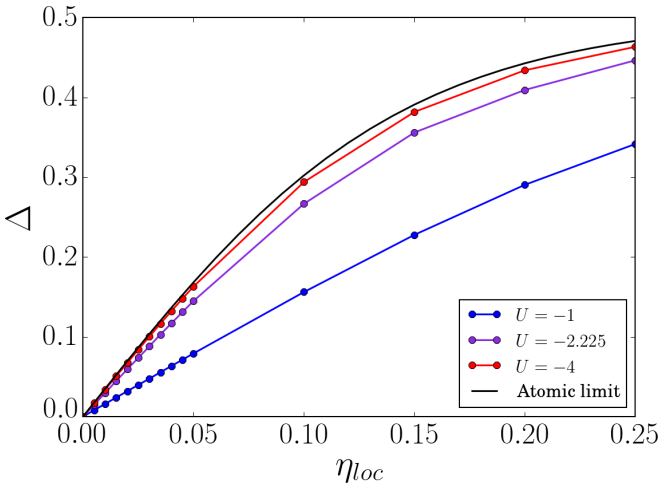

FIG. 4. Local superconducting s-wave order parameter $\Delta = \frac{1}{N}\sum_i \langle c_{i\downarrow} c_{i\uparrow}\rangle$ as a function of the local forcing pairing field η_{loc} in the attractive Hubbard model. The black line provides the analytic behavior in the atomic limit case at $U = -7$ and $\beta = 7$ [see Eq. (9)].

of the pairing field η for the same high temperature ($\beta = 7D^{-1}$). The DMFT behavior of $\Delta(\eta)$ shows quantitative and qualitative differences between the attractive and the repulsive case. The first difference concerns the linear response to the pairing field, which is progressively suppressed by increasing the strength of the repulsive interaction.

Yet, this difference should be considered—from our perspective—only quantitative: Since the linear response is crucially affected by the proximity to the second-order phase transition, it *always* becomes progressively smaller going farther away from the transition (e.g., for the attractive case by increasing T, or for the repulsive case by increasing U). Hence, its absolute value is not *per se* informative about the presence of preformed pairs in the system.

The behavior of the second derivative of $\Delta(\eta)$, instead, is qualitatively richer than in the attractive case (Fig. 3): For small values of η, the second derivative has a positive sign [i.e., $\Delta(\eta)$ is a *convex* function], up to an inflection point η^* (marked by a vertical arrow in the picture). For $\eta > \eta^*$ the curvature becomes negative and $\Delta(\eta)$ becomes concave, approaching eventually the regime value $\Delta = 0.5$.

As a first, heuristic interpretation of this difference, we observe that the appearance of a region with a *convex* curvature at low η reflects the *defiance* of the ($U > 0$) system against the formation of the s-wave pairs induced by the field. Very large fields instead simply override the repulsive interaction leading to the formation of pairs.

This implies a quite general rule of thumb: If, by applying a finite pairing field η to a system of interest, one observes an initial *convex* curvature of the corresponding superconducting response, the presence of an underlying preformed pair physics (with the same symmetry of the pairing field) can be ruled out. In fact, on the basis of our model results, an inspection of sign changes of the second derivative of $\Delta(\eta)$ should provide a good test for detecting the *absence* of preformed pair physics. This rule of thumb, which represents one of the main outcomes of our study, will be applied to the more realistic d-wave pairing in the pseudogap regime of the Hubbard model in Sec. V.

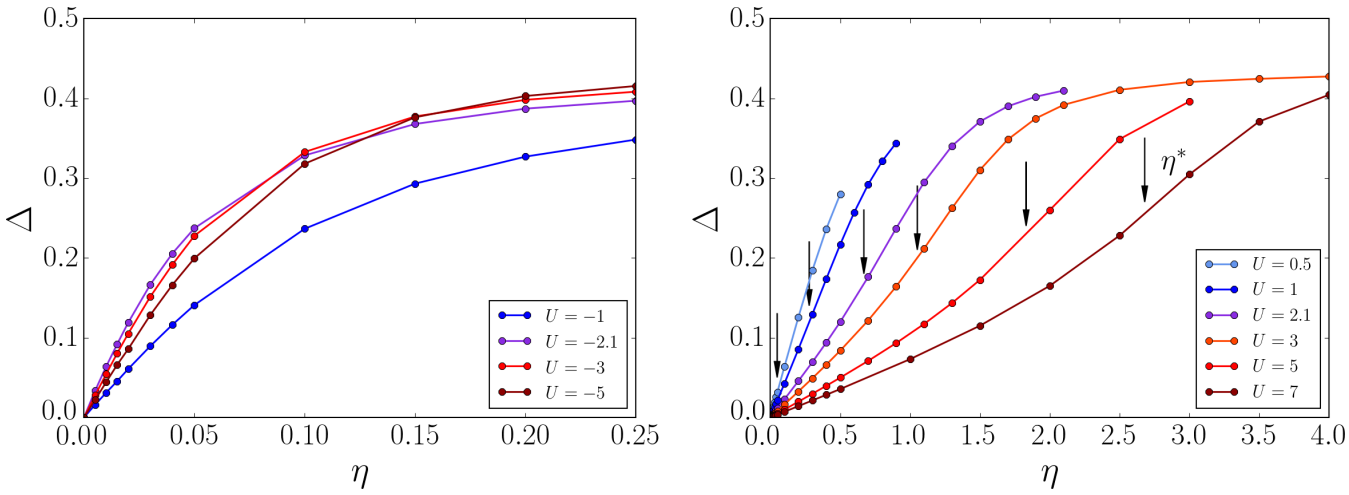

FIG. 5. Superconducting s-wave order parameter $\Delta = \frac{1}{N}\sum_i \langle c_{i\downarrow} c_{i\uparrow}\rangle$ as a function of the forcing pairing field η in the attractive (left panel) and the repulsive (right panel) Hubbard model (at quarter filling). The values of the pairing field corresponding to the inflection point are marked by black arrows.

Before proceeding, however, we should recall that only the first derivative of $\Delta(\eta)$ (and, rigorously, only in the limiting case of $\eta \to 0^+$) has a standard interpretation within the linear response theory. Hence, we need to formalize our heuristic understanding of the curvature of $\Delta(\eta)$ more precisely. This will be done in the next section by investigating explicitly, in relevant limiting cases, the relation between the nature of the ground state of the system and its "defying" response to the pairing field.

B. Quarter-filling study ($n = 0.5$)

The calculations we have presented so far have been performed on the half-filled model. In this section, we repeat the same analysis in the "less symmetric", but more generic, situation of quarter filling ($n = 0.5$).

In Fig. 5 we show the evolution of the s-wave superconducting order parameter Δ as a function for the external field η in the attractive (left panel) and the repulsive (right panel) Hubbard model. In both cases, we observe the same qualitative behavior found at half filling in Fig. 3, with an overall concave $\Delta(\eta)$ for $U < 0$, and an inflection point at η^* for $U > 0$.

The differences with respect to the half-filling case are merely qualitative: For $U < 0$, a weakened response at small η is observed, which is consistent with the suppression of the superconducting order at low densities and with the corresponding atomic limit analysis in Appendix B. For $U > 0$, we find a reduction of η^* with respect to half filling, also consistent with our atomic limit analysis, and coherent with the expected progressive reduction of the effects of the electronic repulsion away from half filling.

Thus, our DMFT analysis at $n = 0.5$, supported by the corresponding atomic limit study in Appendix B, confirms the robustness of the behavior of $\Delta(\eta)$ in a broad range of model parameters and, consequently, the validity of our study also away from the particle-hole symmetric case.

IV. ANALYSIS OF LIMITING CASES

Aiming at extracting the physical information encoded in the second derivative of the superconducting order parameter, we perform an investigation of the simplest limiting cases, i.e., noninteracting ($U = 0$), atomic limit ($t = 0$), and the two-site model, where a full analytical treatment is possible.

We start with the noninteracting case which can be diagonalized in momentum space:

$$H = \sum_{\mathbf{k}\sigma} \epsilon_{\mathbf{k}} c^\dagger_{\mathbf{k}\sigma} c_{\mathbf{k}\sigma} - \eta \sum_{\mathbf{k}} (c^\dagger_{\mathbf{k}\uparrow} c^\dagger_{-\mathbf{k}\downarrow} + c_{-\mathbf{k}\downarrow} c_{\mathbf{k}\uparrow}), \quad (4)$$

where $\epsilon_{\mathbf{k}}$ represents the free-particle energy dispersion. Because of the presence of the static field η, one immediately recognizes the formal analogy with the BCS mean field. After a few algebraic steps (see Appendix A), one obtains

$$\Delta(\eta) = \frac{\eta}{\pi D^2} \int_{-D}^{D} d\epsilon \frac{\sqrt{D^2 - \epsilon^2}}{\sqrt{\epsilon^2 + \eta^2}} \tanh\left(\frac{\beta\sqrt{\epsilon^2 + \eta^2}}{2}\right). \quad (5)$$

While this integral can be computed numerically, it is insightful to study its behavior in the zero and high-temperature regimes for a small pairing field ($\eta \ll 1$ and $\beta\sqrt{\eta^2 + \epsilon^2} \ll 1$). In the first case, we have

$$\begin{aligned}\Delta(\eta)|_{T=0} &= \frac{2\eta}{\pi}\left[\int_0^\eta d\epsilon \frac{\sqrt{1-\epsilon^2}}{\sqrt{\epsilon^2+\eta^2}} + \int_\eta^1 d\epsilon \frac{\sqrt{1-\epsilon^2}}{\sqrt{\epsilon^2+\eta^2}}\right] \\ &\simeq \frac{2\eta}{\pi}\left[\frac{\eta^2}{2} + \ln(2) - \ln(\eta)\right]. \end{aligned} \quad (6)$$

Hence, at $T = U = 0$, the first derivative exhibits a positive logarithmic divergence as $\eta \to 0$, which is readily understood by looking at the noninteracting problem in the limit of vanishing interaction ($U/D \to 0$). Since T_c decreases exponentially as $U \to 0$ [1], the noninteracting pair susceptibility at $U = 0$ must diverge exactly at $T = 0$. In the opposite, high-temperature regime, the expansion of the Fermi function as $\beta\sqrt{\eta^2 + \epsilon^2} \ll 1$ yields

$$\Delta(\eta) \simeq \frac{\beta}{4}\eta - \frac{\beta^2\eta}{4\pi}\int_0^1 d\epsilon \sqrt{1-\epsilon^2}\sqrt{\epsilon^2+\eta^2}. \quad (7)$$

As the second integral is always positive, we obtain an overall *negative* value of the second derivative of Δ, which vanishes

only for $\eta \to 0$. The study of the noninteracting case is not fully conclusive in itself, but it already indicates that a *negative* curvature of $\Delta(\eta)$ does not provide an unambiguous indication of an underlying preformed pair physics, certainly absent in our model for $U = 0$.

Further insights can be gained by considering the atomic limit ($t = 0$) of Eq. (1). Here, the superconducting order parameter assumes the following expression (see Appendix B):

$$\Delta(\eta) = \frac{\eta}{2\,\epsilon}\,\frac{\sinh(\beta\epsilon)}{\cosh(\beta\epsilon) + e^{\beta\frac{U}{2}}}, \tag{8}$$

where $\epsilon = \sqrt{\mu^2 + \eta^2}$. In particular, Eq. (8) further simplifies at half filling:

$$\Delta_{\rm att}(\eta) = \frac{1}{2}\,\frac{\sinh(\beta\eta)}{\cosh(\beta\eta) + e^{-\beta\frac{|U|}{2}}}, \tag{9}$$

$$\Delta_{\rm rep}(\eta) = \frac{1}{2}\,\frac{\sinh(\beta\eta)}{\cosh(\beta\eta) + e^{\beta\frac{|U|}{2}}}, \tag{10}$$

whose dependence on η, at different temperatures, is plotted in Fig. 6 both for the attractive and the repulsive case. By exploiting a (rather rough) resemblance of the $\Delta(\eta)$ curves to the corresponding DMFT results of Fig. 3, we progress in clarifying the physical meaning of the second derivative of $\Delta(\eta)$. In particular, let us now focus on the repulsive atomic case, whose $\Delta(\eta)$ displays an inflection point at $\eta^* = U/2$, in a somewhat similar fashion to the DMFT results. We observe that the inflection point η^* is exactly associated with a corresponding change of the ground state. By diagonalizing the Hamiltonian (see Appendix B), a crossing of energy levels occurs exactly at $\eta^* = U/2$: For $\eta < \eta^*$ the lowest energy eigenvalue is achieved in the (degenerate) subspace $\{|\uparrow\rangle, |\downarrow\rangle\}$ describing an (isolated) magnetic moment, while for $\eta > \eta^*$, the ground state becomes $\frac{|\uparrow\downarrow\rangle + |0\rangle}{\sqrt{2}}$, i.e., a doubly/empty occupied state. Hence, the curvature of the superconducting response, as a function of the pairing field, provides direct information about the ground-state properties of the system and, in particular, about the presence or the absence of pairs.

The simplest way to verify to what extent these results hold, also for *finite* electron hopping, is to consider a two-site model. Here the Hilbert space is spanned by 16 basis vectors and the matrix can be readily diagonalized (see Appendix C), allowing us to exactly compute the ground-state vector and Δ (Fig. 7) as a function of η.

The agreement with DMFT obviously improves with respect to the atomic limit and an inflection point at η^* remains well visible. The broadening around the inflection point is no longer just a mere effect of the temperature as in the atomic case, but it results from the interplay between the magnetic moment and pair formation tendencies of the ground state. Such interplay is—evidently—affected by the hopping term, as also happens for the DMFT results.

Also in this case we relate $\Delta(\eta)$, and specifically, the value of its inflection point η^*, to the corresponding evolution of the system's ground state. For the latter, in the presence of the

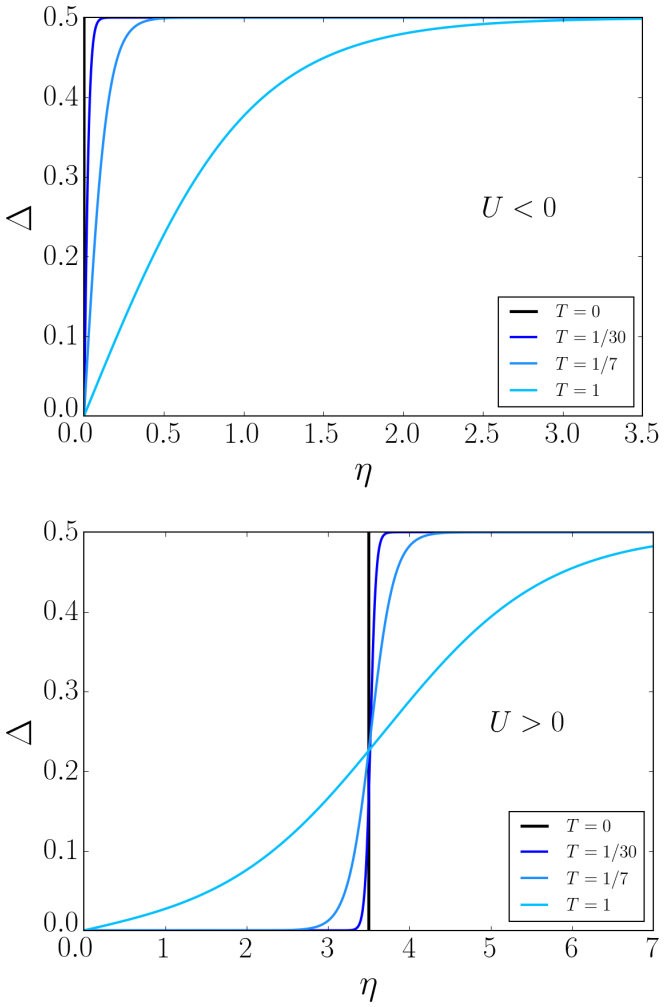

FIG. 6. Analytic behavior in the atomic limit of the superconducting order parameter $\Delta = \frac{1}{N}\sum_i \langle c_{i\downarrow} c_{i\uparrow}\rangle$ with respect to the forcing pairing field η in the attractive (upper panel) and in the repulsive (lower panel) Hubbard model for $U = -7$ (and $U = 7$ in the repulsive case) and different temperature values [see Eqs. (9) and (10)].

pairing field η, we obtain

$$|\mathrm{GS}\rangle = \alpha\left(\frac{|\uparrow,\downarrow\rangle - |\downarrow,\uparrow\rangle}{\sqrt{2}}\right) + \beta\left(\frac{|\uparrow\downarrow,0\rangle + |0,\uparrow\downarrow\rangle}{\sqrt{2}}\right) + \gamma\left(\frac{|0,0\rangle + |\uparrow\downarrow,\uparrow\downarrow\rangle}{\sqrt{2}}\right), \tag{11}$$

where the coefficients α, β, γ vary continuously as a function of the field η and the interaction strength U. The first term of Eq. (11) represents a singlet state over the two sites while the two remaining terms feature empty and double occupations. Intuitively, the singlet state could be linked to the presence of a localized magnetic moment (with antiferromagnetic tendency) in the ground state, while the other states contain localized ("preformed") pairs.

The explicit dependence of the squared amplitude of α, β, γ is shown in Fig. 8 as a function of the pairing field and for different values of the interaction U: The coefficients show a smooth evolution as a function of η which becomes sharper by increasing the interaction, before recovering the

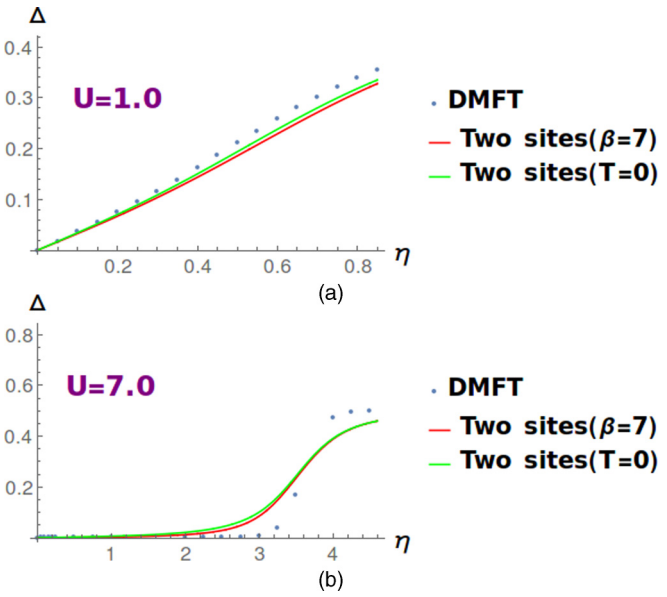

FIG. 7. Superconducting order parameter $\Delta(\eta) = \frac{1}{N}\sum_i \langle c_{i\downarrow} c_{i\uparrow}\rangle$ as a function of η: comparison between the DMFT results at $\beta = 7D^{-1}$ and the two-site results for $T = 0$ (green line) and $\beta = 7D^{-1}$ (red line).

step function of the atomic limit for $U \to \infty$. For any given value of U, $|\alpha|^2$ monotonically increases with η, while $|\beta|^2$ and $|\gamma|^2$ decrease, reflecting the progressively enhanced weight of "pairs" (doubly occupied sites) induced by the pairing field.

By reporting the corresponding values of the inflection point η^* (as extracted by the data of Fig. 7) we find that η^* occurs in correspondence of the value of $|\alpha|^2 = 0.5$ (marked by dashed line in the figure) in the intermediate- and strong-coupling regimes ($U = 3$ and $U = 7$). This reflects the fact that, *also* in the two-site model, the sign change of the second derivative of $\Delta(\eta)$ marks a change of the prevalent character of the ground state. This is dominated by localized magnetic moments ($|\alpha|^2 > 0.5 > |\beta|^2 + |\gamma|^2$) for $\eta < \eta^*$, i.e., where the curvature of $\Delta(\eta)$ is convex. On the other hand, local ("preformed") pairs prevail ($|\alpha|^2 < 0.5 < |\beta|^2 + |\gamma|^2$) for $\eta > \eta^*$, i.e., where a concave curvature of $\Delta(\eta)$ occurs. Our microscopic analysis confirms thus the link between the curvature of $\Delta(\eta)$ with the tendency of the system to contrast or to favor the driven superconducting state.

From a quantitative perspective, one should note that in the weak-coupling regime [$U = 1$, Fig. 8(a)], the inflection point η^* is slightly before the coefficient $|\alpha|^2$ crosses the value 0.5; i.e., at $\eta = \eta^*$ one finds an $|\alpha|^2$ slightly larger than 0.5. While this weak-coupling feature might be a specific result of the two-site model, its presence does not compromise the validity of our interpretation. This can be better understood looking at Fig. 10, where the physics of the two-site model with the pairing field is eventually summarized. Here, in a phase diagram U vs η (drawn at a fixed $T = 1/7D$), the values of η^* and of the loci where $|\alpha|^2 = 0.5$ are reported. Moreover, in the spirit of Sec. II, different region of the phase diagram could be defined, and classified in terms of the kinetic/potential energy gain/losses induced by the application of the (finite) pairing

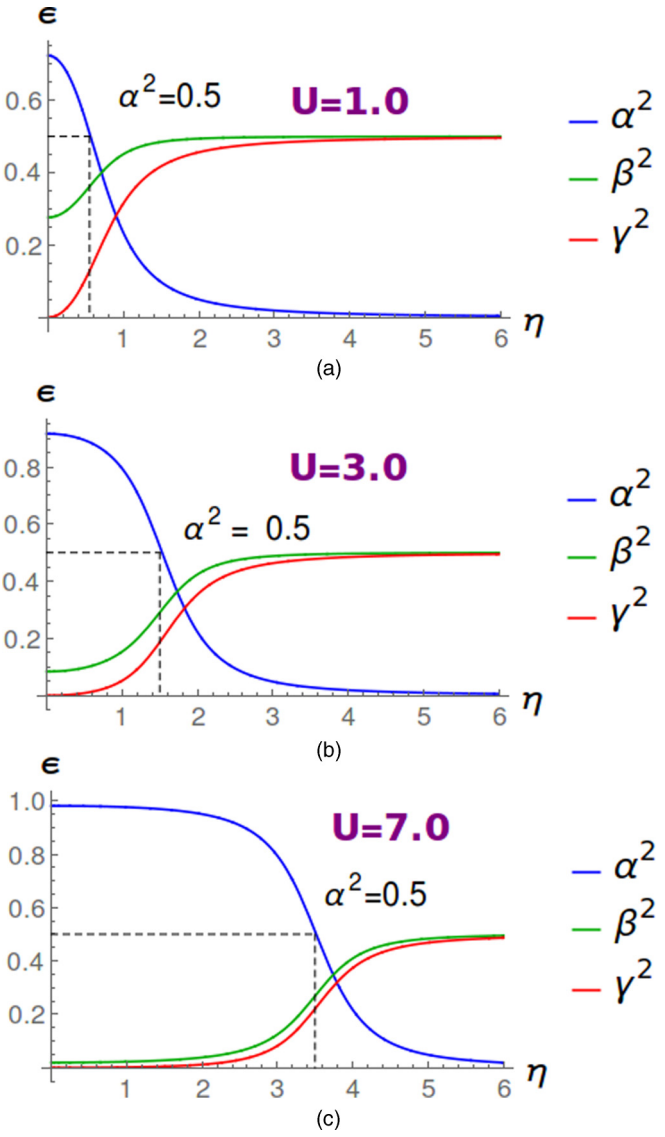

FIG. 8. Ground-state coefficients $|\alpha|^2$ (blue line), $|\beta|^2$ (green line), and $|\gamma|^2$ (red line) of the two-site model [Eq. (11)] for different U values as a function of the forcing field η.

field:

$$\begin{aligned} \langle H_{\rm K}\rangle_\eta - \langle H_{\rm K}\rangle_{\eta=0} &= -2\alpha\beta + \frac{2}{U}\left(1+\frac{4}{U^2}\right)^{1/2}, \\ \langle H_{\rm pot}\rangle_\eta - \langle H_{\rm pot}\rangle_{\eta=0} &= -U\alpha^2 - 4\eta\beta\gamma \\ &\quad + \frac{U}{2}\left[1+\left(1+\frac{4}{U^2}\right)^{-1/2}\right]. \end{aligned} \tag{12}$$

The energetic balance analysis of Fig. 10 confirms, hence, that the correspondence between η^* and the change of nature in the ground state of the two-site model is rather solid in the whole intermediate and BEC coupling regime (relevant for the preformed pair physics) with minor deviations occurring in the BCS regime. Moreover, we observe that in the BCS region for $\eta = \eta^*$, $|\alpha|^2$ is slightly larger than 0.5, indicating that a convex (=positive) curvature of $\Delta(\eta)$ is definitely *incompatible* with any preformed pair physics

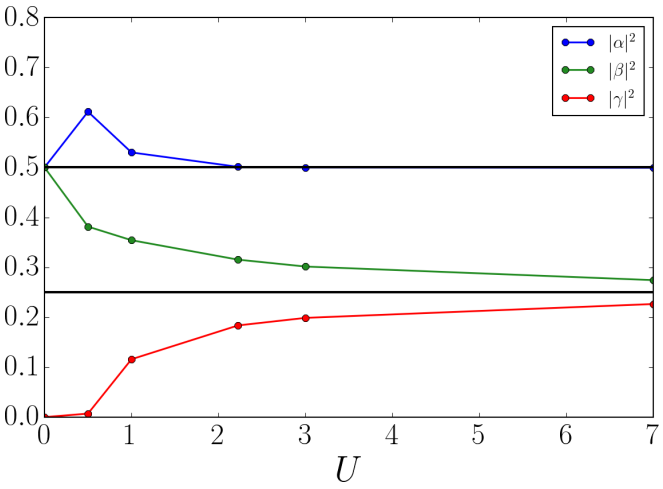

FIG. 9. Values of the coefficients $|\alpha|^2$, $|\beta|^2$, and $|\gamma|^2$ of Eq. (11) at η^* as a function of U.

in the ground state (see Figs. 9 and 10). We finally note that such criterion of "absence", usable to rigorously exclude the presence of preformed pairs, is also compatible with the analysis of the concave (=negative) curvature of $\Delta(\eta)$ in the noninteracting case, discussed at the beginning of the section.

V. IMPLICATIONS FOR OTHER STUDIES

By analyzing systematically the superconducting response (Δ) of simple models to an external s-wave pairing field (η), we have demonstrated that, whenever $\Delta(\eta)$ displays a *convex* curvature in the low-field limit, we can safely exclude preformed Cooper pairs. In this section, we discuss the relevance of this rule-of-thumb criterion to a wider range of systems. Through a unitary transformation, the pairing field and the superconducting order parameter in the attractive Hubbard model map onto the magnetic field and the magnetic

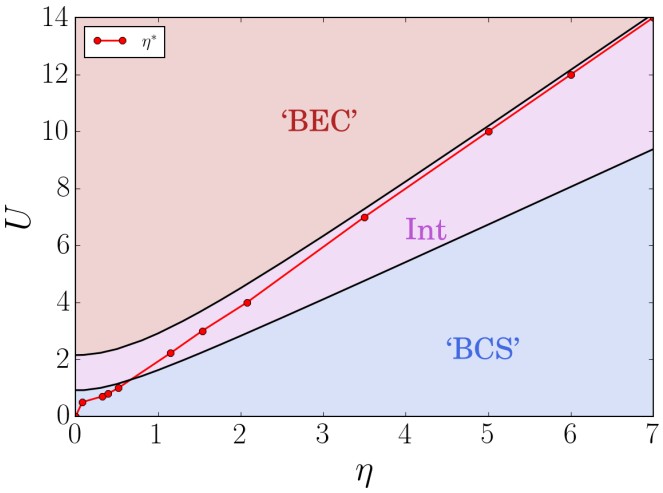

FIG. 10. U-η plane showing the different regimes obtained from an energy balance analysis in the two-site model. The blue, violet, and red regions indicate respectively the weak-, intermediate-, and strong-coupling regimes. The η^* behavior at different U values is shown by the red line.

moments in the correspondent repulsive counterpart [2]. This means that our findings apply also for detecting the presence/absence of preformed magnetic moments by means of an external magnetic field. This generalization of our results is particularly promising, because a measure of the magnetization as a function of the magnetic field is obviously not a pure theoretical probe and it can be directly exploited in various experiments (at least for the study of preformed moments in ferromagnetic compounds).

Since the presence and the role of preformed magnetic moments remain a debated issue for several correlated materials, ranging from simple metals such as Fe and Ni [42–45] to alloys (FeAl [46]) and iron-pnictides and chalcogenides [47,48], the clear-cut criterion proposed in this work may find widespread application in future experimental and theoretical studies of these materials.

One may also envisage further applications of our results as an idealized description of pump-probe experiments on superconductors. There, a transient state with an optical response, which is at least compatible with a superconductor, can be created by impulsive excitations inducing coherent phonon deformations, while leaving the temperature of the electrons unchanged [49–53]. Comparing experiments against our idealized calculations, one could analyze to which extent the impulsive excitation can be interpreted as an external field driving superconductivity (obviously in our calculations the driven superconductivity is static, as the external field does not depend on time).

One of the most natural applications of our results is, however, the possible presence of preformed d-wave pairs in the pseudogap phase of the two-dimensional Hubbard model. Indeed a closely related theoretical analysis has already been performed using the dynamical cluster approximation (DCA) [54], an extension of DMFT where the single impurity is replaced by a cluster of N_c sites. An external d-wave pairing field was applied and the resulting d-wave superconducting response $\Delta_{\mathbf{k}}$ was then computed [15]. Without driving fields, for $N_c = 8$ and $U > 1.5D$ (with $D = 4t$) the superconducting phase is replaced by the pseudogap state, where a strong spectral weight suppression is found at the antinodal point, without any superconducting long-range order. Clearly, the identification of the physical origin of this phase is also crucial to understand the debated underlying physics of the high-temperature superconductors. In this respect, the two main alternative interpretations describe the pseudogap either as the result of intrinsic interaction effects (spin fluctuations, Mott physics, or other) or as the signature of preformed d-wave pairs.

The results of Ref. [15] are reproduced in Fig. 11, which shows $\Delta_{\mathbf{k}}(\eta_{\mathbf{k}})|_{\mathbf{k}=(0,\pi)}$ as a function of the external d-wave pairing field field $\eta = \eta_d$. On the basis of these calculations the authors concluded that the superconducting response to a d-wave forcing field was "weak enough" to exclude a preformed pair origin of the pseudogap state in DCA. This statement is certainly reasonable, but it still lacks formal strength as it is not based on some precise criterion.

A closer look to the data of Fig. 11 shows that, besides an expected progressive suppression of the linear response moving away from the critical regime, one observes a sign change of the second derivative of $\Delta_{\mathbf{k}}(\eta_d)$, which starts

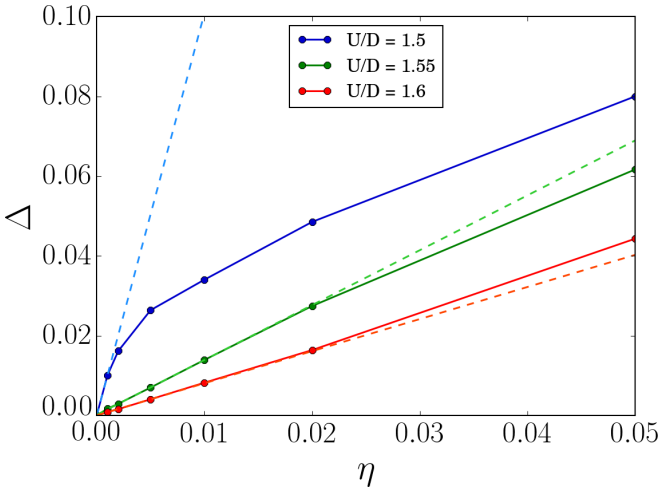

FIG. 11. (DCA data reproduced from Ref. [15].) The d-wave superconducting order parameter induced by the corresponding d-wave pairing field η_d: in a DCA calculation for a 2D Hubbard model at $\beta D = 240$ the order parameter $\Delta_{\mathbf{k}}$ is evaluated in the sector $\mathbf{k} = (0,\pi)$ and plotted as a function of η_d at doping $x = 0$ for interaction strengths indicated. The dashed lines, marking the slope of the (linear) response at $\eta_d \to 0^+$, make more easily noticeable the curvature change of $\Delta(\eta_d)$ occurring for the data set at $U = 1.6D$.

displaying a convex curvature for small fields at $U = 1.6D$. Hence, according to our criterion, we can now safely conclude that, once the system is sufficiently far from the superconducting instability, there are no well-defined preformed pairs which couple with the external pairing field in a parameter region where the pseudogap is observed in DCA. This excludes a preformed-pair origin of the pseudogap and it is rather suggestive of a major role played by the strong antiferromagnetic correlations or by nonlocal Mott physics. It is worth mentioning that the claim of a lack of preformed pairs of Ref. [15], made more rigorous by the present analysis, is not necessarily in contradiction with the claim, based on a different DCA study [16], of significant d-wave pairing fluctuations also far from T_c. The latter result indeed refers to *short-ranged* fluctuations both in space and time, while the (static) forcing-field analysis focuses on long-lived pairs. Indeed these results are perfectly compatible in view of the more recent study of Ref. [17], where it has been shown that well-defined spin fluctuations, emerging as the predominant pseudogap mechanism according to our analysis of the data of Ref. [15], show up as short-range/short-lived pairing fluctuating modes, if viewed from the perspective of the particle-particle scattering channel.

VI. CONCLUSIONS

This work has been devoted to the definition of an operative criterion to confirm or exclude the existence of preformed pairs in a non-superconducting state. This goal has been achieved by a systematic DMFT study of the response to an external s-wave pairing forcing field η in the controlled situation of a single band (attractive and repulsive) Hubbard model. For strong attractive interactions we are indeed certain of the existence of a preformed pair region, while the repulsive model does not host any s-wave pair.

By comparing the different regimes, we identified a clear-cut rule-of-thumb criterion for excluding a preformed pair physics: The latter are certainly absent, if the second derivative of $\Delta(\eta)$ is positive in a finite region of η from 0 to a finite value η^* [i.e., $\Delta(\eta)$ is a convex function at small fields]. This happens because the convexity of $\Delta(\eta)$ reflects the "reluctance" of the systems to respond to the pairing field. In other words, the positive second derivative indicates that the applied forcing field is not intense enough to *revert* the dominant nature of the ground state, which is opposed to the order induced by the probing field. Only if η is enough large to exceed any intrinsic property of the model, the curvature changes sign and becomes concave, leading, eventually, to a saturation to the maximum pairing amplitude. This behavior testifies to the absence of any intrinsic preformed pairing.

On the other hand, an overall concave curvature of $\Delta(\eta)$ is a necessary condition for the existence of preformed pairs, but it is not a sufficient condition. Therefore, the latter should be supplemented with further physical information, such as the energetic balance underlying superconductivity, as we also discuss in Sec. II of this paper.

Our results have a potential impact for several different aspects. Our rule of thumb can be indeed applied, as showed in the previous section, for improving the interpretation of cutting-edge DCA calculations [15], relevant for the cuprate physics, and—in particular—to exclude on a rigorous basis that the pseudogap state of DCA is originated by preformed pair fluctuations. Indeed, a related analysis has been proposed in Ref. [15], where, however, the physical interpretation of the results was mostly heuristic.

Moreover, it is quite natural to extend the conclusions of our analysis (and, in particular, our criterion) to cases of other, more physical, forcing fields: This would be, e.g., the case of a (finite) magnetic field exploited to detect preformed magnetic moments via the evolution of the magnetization as a function of magnetic field beyond linear response. Evidently, the latter analysis allows also for direct experimental realizations.

Finally, we notice that the study of regimes of external perturbation field, far away from the linear response, might provide important complementary information to interpret more challenging nonequilibrium phenomena. Comparing our results with pump-probe experiments where transient superconductivity is realized by coherently exciting phonon modes, we could study whether, and to which extent, these nonequilibrium phenomena can be interpreted in terms of a light-driven pairing field which favors pair formation.

ACKNOWLEDGMENTS

We thank E. Gull, O. Gunnarsson, C. Taranto, G. Sangiovanni, T. Schäfer, and G. Rohringer for insightful discussions. We acknowledge financial support for our research activities from the Austrian Science Fund (FWF) through the project I-610-N16 and the subproject I-1395-N16 as part of the German Research Foundation (DFG) research unit FOR 1346.

APPENDIX A: NONINTERACTING CASE

The half-filled noninteracting problem under a isotropic pairing forcing field η can be easily solved in $\mathbf{k}$ space. Here, the Hamiltonian assumes the following form:

$$H = \sum_{\mathbf{k}\sigma} \epsilon_{\mathbf{k}} c^{\dagger}_{\mathbf{k}\sigma} c_{\mathbf{k}\sigma} - \eta \sum_{\mathbf{k}} (c^{\dagger}_{\mathbf{k}\uparrow} c^{\dagger}_{-\mathbf{k}\downarrow} + c_{-\mathbf{k}\downarrow} c_{\mathbf{k}\uparrow}), \tag{A1}$$

where $\epsilon_{\mathbf{k}}$ represents the free particle energy dispersion. This Hamiltonian can be exactly diagonalized by exploiting the Bogoliubov transformations [1], which read

$$\begin{cases} \gamma^{\dagger}_{\mathbf{k},\uparrow} = u_{\mathbf{k}} c_{\mathbf{k},\sigma}{}^{\dagger} - v_{\mathbf{k}} c_{-\mathbf{k},\downarrow}, \\ \gamma_{-\mathbf{k},\downarrow} = u_{\mathbf{k}} c_{-\mathbf{k},\downarrow} + v_{\mathbf{k}} c_{\mathbf{k},\uparrow}{}^{\dagger}, \end{cases} \tag{A2}$$

where

$$\begin{cases} u_{\mathbf{k}}^2 = \frac{1}{2}\left(1 + \frac{\epsilon(\mathbf{k})}{E(\mathbf{k})}\right), \\ v_{\mathbf{k}}{}^2 = \frac{1}{2}\left(1 - \frac{\epsilon(\mathbf{k})}{E(\mathbf{k})}\right), \end{cases} \tag{A3}$$

and $E(\mathbf{k}) = \sqrt{\epsilon_{\mathbf{k}}{}^2 + \eta^2}$.

In order to evaluate the superconducting order parameter in real space, one has to perform the expectation value of the annihilation "pair operator" $b_{\mathbf{k}} = c_{-\mathbf{k}\downarrow} c_{\mathbf{k}\uparrow}$ and sum over the Brillouin zone:

$$\begin{aligned} \langle b_{\mathbf{k}} \rangle &= \langle c_{-\mathbf{k}\downarrow} c_{\mathbf{k}\uparrow} \rangle = u^*_{\mathbf{k}} v_{\mathbf{k}} (1 - \langle \gamma_{\mathbf{k}\uparrow}{}^{\dagger} \gamma_{\mathbf{k}\uparrow} \rangle - \langle \gamma_{\mathbf{k}\downarrow}{}^{\dagger} \gamma_{\mathbf{k}\downarrow} \rangle) \\ &= u^*_{\mathbf{k}} v_{\mathbf{k}} [1 - 2 f(E_{\mathbf{k}})], \end{aligned} \tag{A4}$$

where $f(E_{\mathbf{k}})$ represents the usual Fermi-Dirac thermal distribution for fermion-like excitations with energy $E_{\mathbf{k}}$. Hence, we finally end up with the following expression for the superconducting order parameter:

$$\begin{aligned} \Delta &= \sum_{\mathbf{k}} u^*_{\mathbf{k}} v_{\mathbf{k}} [1 - 2 f(E_{\mathbf{k}})] \\ &= \sum_{\mathbf{k}} \frac{\eta}{2E(\mathbf{k})} [1 - 2 f(E_{\mathbf{k}})] \\ &= \frac{\eta}{2} \int_{-D}^{D} d\epsilon \frac{D(\epsilon)}{E(\epsilon)} [1 - 2 f(E(\epsilon))]. \end{aligned} \tag{A5}$$

Explicitly substituting the DOS of the Bethe-lattice and the Fermi-Dirac thermal distribution, one gets Eq. (5).

APPENDIX B: ATOMIC LIMIT

In this section we explicitly derive the expression for the superconducting order parameter Δ in the atomic limit. We proceed in two steps: first we perform the unitary transformation to map the attractive Hubbard model onto the repulsive one; second we project the system onto the new principal axes and evaluate the expectation value $\langle c_{i\downarrow} c_{i\uparrow} \rangle$ in the starting (attractive) system. Note that the analogous procedure can be adopted for the repulsive case just by swapping the U sign.

Let us start from the attractive Hubbard model Hamiltonian, properly readjusted to emphasize the particle-hole symmetry:

$$\begin{aligned} H_{attr} = U \sum_i \left(n_{i\uparrow} - \frac{1}{2}\right)\left(n_{i\downarrow} - \frac{1}{2}\right) - \left(\mu - \frac{U}{2}\right) \\ \times \sum_i (n_{i\uparrow} + n_{i\downarrow}) - \eta \sum_i (c^{\dagger}_{i\uparrow} c^{\dagger}_{i\downarrow} + \text{H.c.}). \end{aligned} \tag{B1}$$

Here $U < 0$ and μ is the shifted chemical potential (note $\mu = U/2$ at half filling). By performing the unitary transformation to map the attractive Hubbard model onto the repulsive one [2],

$$\begin{cases} c_{i\downarrow} \to (-1)^{n_i} c^{\dagger}_{i\downarrow}, \\ c_{i\uparrow} \to c_{i\uparrow}, \end{cases} \tag{B2}$$

we end up with the corresponding repulsive Hubbard Hamiltonian:

$$\begin{aligned} H_{rep} = |U| \sum_i n_{i\uparrow} n_{i\downarrow} - \frac{|U|}{2} \sum_i (n_{i\uparrow} + n_{i\downarrow}) - \left(\mu + \frac{|U|}{2}\right) \\ \times \sum_i (n_{i\uparrow} - n_{i\downarrow}) - \eta \sum_i (-1)^{n_i} (c^{\dagger}_{i\uparrow} c_{i\downarrow} + c^{\dagger}_{i\downarrow} c_{i\uparrow}). \end{aligned} \tag{B3}$$

Notice that Eq. (B3) is nothing but a half-filled repulsive system with two external magnetic fields applied onto the z and the x axes. Since the first two terms are invariant under axis rotation, it is convenient to perform a unitary transformation of the operators, projecting the system along the principal axes in the (x,z) plane.

Diagonalizing the last two terms in the 4-state Hilbert space for the single site and making the proper transformations, we end up with to the following expression:

$$\begin{aligned} H_{rep} = |U| \sum_i n_{i\uparrow} n_{i\downarrow} - \frac{|U|}{2} \sum_i (n_{i\uparrow} + n_{i\downarrow}) \\ + \epsilon \sum_i (n_{i\uparrow} - n_{i\downarrow}), \end{aligned} \tag{B4}$$

where $\epsilon = \sqrt{(\mu + \frac{|U|}{2})^2 + \eta^2}$ is the effective magnetic field resulting from the μ and η terms.

In order to evaluate the superconducting order parameter Δ, we need to map the pairing operator $c_{i\downarrow} c_{i\uparrow}$ onto the corresponding repulsive system by projecting it along the principal axes. We obtain

$$\begin{aligned} \langle c_{i\downarrow} c_{i\uparrow} \rangle \to \frac{1}{4\eta\epsilon^2} \Bigg[-\frac{\left(\epsilon - \frac{|U|}{2} - \mu\right)}{a^2} \langle c^{\dagger}_{i\uparrow} c_{i\uparrow} \rangle \\ + \frac{\left(\epsilon + \frac{|U|}{2} + \mu\right)}{b^2} \langle c^{\dagger}_{i\downarrow} c_{i\downarrow} \rangle \Bigg], \end{aligned} \tag{B5}$$

where $a/b = [\eta^2 + (\mu \pm \frac{|U|}{2} \pm \epsilon)]^{-1/2}$.

Evaluating explicitly the expectation values in Eq. (B5) one obtains

$$\Delta(\eta) = \frac{\eta}{2\,\epsilon} \frac{\sinh(\beta\epsilon)}{\cosh(\beta\epsilon) + e^{-\beta \frac{|U|}{2}}}, \tag{B6}$$

which reduces to the simpler expression in the half-filling case:

$$\Delta_{\rm att}(\eta) = \frac{1}{2}\,\frac{\sinh(\beta\eta)}{\cosh(\beta\eta) + e^{-\beta\frac{|U|}{2}}}. \tag{B7}$$

Since this expression is typically applicable for large values of $|U|$, one can notice that the order parameter exhibits a weak dependence on the interacting constant. This also sets a minimum value for the slope in the limit $|U| \to +\infty$ at finite temperature:

$$\lim_{|U|\to+\infty} \left.\frac{\partial\Delta_{\rm att}}{\partial\eta}\right|_{\eta=0} = \frac{\tanh\left(\beta\left|\mu + \frac{|U|}{2}\right|\right)}{2\left|\mu + \frac{|U|}{2}\right|}, \tag{B8}$$

which displays a maximum in the half-filling case:

$$\lim_{|U|\to+\infty} \left.\frac{\partial\Delta_{\rm att}}{\partial\eta}\right|_{\eta=0,\mu=-\frac{|U|}{2}} = \frac{\beta}{2}. \tag{B9}$$

This means that, away from half-filling, the superconducting linear response of the system is progressively reduced and, thus, the regime value $\Delta = 0.5$ is approached more slowly if compared with the half-filling situation. This result is consistent with the DMFT data shown in Fig. 5 (left panel). A study on the second derivative $\partial^2\Delta_{\rm att}/\partial\eta^2$ shows that, for all $\eta > 0$, the superconducting order parameter exhibits a negative curvature in the attractive Hubbard model, as shown in Fig. 6 for the half-filling case (upper panel). The corresponding behavior for $U > 0$ (in the half-filling case) is shown in Fig. 6 (lower panel).

Ground state

As a final atomic limit analysis in the repulsive case, we can look at the ground-state evolution as a function of the external pairing field. The local, repulsive Hamiltonian has the following form:

$$H^i_{rep} = U\, n_{i\uparrow}n_{i\downarrow} - \frac{U}{2}\,(n_{i\uparrow} + n_{i\downarrow}) - \eta\,(c_{i\downarrow}c_{i\uparrow} + c^\dagger_{i\uparrow}c^\dagger_{i\downarrow}), \tag{B10}$$

where, for the sake of simplicity, we reduced at half filling.

By diagonalizing the 4×4 block matrix, we find three different eigenvalues: $-U/2$ (twofold degenerate), $\pm\eta$. Therefore, as soon as $\eta \to U/2$, the ground state of the system abruptly changes from the degenerate subspace to the eigenstate associated with $-\eta$, namely,

$$|-\eta\rangle = \frac{|\uparrow\downarrow\rangle + |0\rangle}{\sqrt{2}}. \tag{B11}$$

Out of half filling the condition for having this level crossing which changes abruptly the ground state of the system from singly occupied magnetic moment to $\frac{|\uparrow\downarrow\rangle+|0\rangle}{\sqrt{2}}$ becomes

$$\sqrt{\eta^2 + \left(\mu - \frac{U}{2}\right)^2} = \frac{U}{2}. \tag{B12}$$

Although μ depends in general on the specific parameters of the system (e.g., temperature, electronic density, and external field η) and it must be determined self-consistently, it is clear from Eq. (B12) that the change of the ground state will occur at a smaller value of the pairing field η than the half-filled system. This trend is also coherent with the DMFT results in Fig. 5 (right panel).

APPENDIX C: TWO-SITE MODEL

In this section we target the solution of the repulsive Hubbard model taking into account just two sites. The two-site Hamiltonian reads

$$H = -t\sum_\sigma (c^\dagger_{1\sigma}c_{2\sigma} + c^\dagger_{2\sigma}c_{1\sigma}) + U\sum_{i=1,2}\left(n_{i\uparrow} - \frac{1}{2}\right) \times \left(n_{i\downarrow} - \frac{1}{2}\right) - \eta\sum_{i=1,2}(c^\dagger_{i\uparrow}c^\dagger_{i\downarrow} + c_{i\downarrow}c_{i\uparrow}), \tag{C1}$$

where t is the hopping integral, $U > 0$ is the interaction parameter, and η represents the external pairing field. Since we are working in the grand-canonical ensemble, the Hilbert space is spanned by 16 basis vectors, namely,

$$\{|\uparrow,\downarrow\rangle,|\downarrow,\uparrow\rangle,|\uparrow\downarrow,0\rangle,|0,\uparrow\downarrow\rangle,|\uparrow,\uparrow\rangle,|\downarrow,\downarrow\rangle\} \Rightarrow \text{ssp } n = 1, \tag{C2}$$

$$\{|\uparrow,0\rangle,|\downarrow,0\rangle,|0,\uparrow\rangle,|0,\downarrow\rangle\} \Rightarrow \text{ssp } n = 0.5, \tag{C3}$$

$$\{|\uparrow,\uparrow\downarrow\rangle,|\downarrow,\uparrow\downarrow\rangle,|\uparrow\downarrow,\uparrow\rangle,|\uparrow\downarrow,\downarrow\rangle\} \Rightarrow \text{ssp } n = 1.5, \tag{C4}$$

$$\{|\uparrow\downarrow,\uparrow\downarrow\rangle\} \Rightarrow \text{ssp } n = 2, \tag{C5}$$

$$\{|0,0\rangle\} \Rightarrow \text{ssp } n = 0, \tag{C6}$$

where each line indicates a specific subspace (ssp) characterized by an electron density n. By exploiting the symmetries of the system one can identify for which states the Hamiltonian is diagonal:

$$\left\{\frac{|\uparrow\downarrow,0\rangle - |0,\uparrow\downarrow\rangle}{\sqrt{2}}, \frac{|0,0\rangle - |\uparrow\downarrow,\uparrow\downarrow\rangle}{\sqrt{2}}\right\} \Rightarrow E_1 = 0, \tag{C7}$$

$$\left\{|\uparrow,\uparrow\rangle,|\downarrow,\downarrow\rangle,\frac{|\uparrow,\downarrow\rangle + |\downarrow,\uparrow\rangle}{\sqrt{2}}\right\} \Rightarrow E_2 = -U, \tag{C8}$$

while projecting the Hamiltonian on the 3-dimensional subspace $\{\frac{|0,0\rangle+|\uparrow\downarrow,\uparrow\downarrow\rangle}{\sqrt{2}}, \frac{|\uparrow\downarrow,0\rangle+|0,\uparrow\downarrow\rangle}{\sqrt{2}}, \frac{|\uparrow,\downarrow\rangle-|\downarrow,\uparrow\rangle}{\sqrt{2}}\}$ gives the following matrix:

$$M = \begin{pmatrix} -U & -2t & 0 \\ -2t & 0 & -2\eta \\ 0 & -2\eta & 0 \end{pmatrix}. \tag{C9}$$

One can demonstrate that this matrix has three distinguished real eigenvalues (E_3, E_4, and E_5) even if an explicit simple expression cannot be found analytically. Nevertheless, we are able to compute numerically eigenvalues and eigenvectors as a function of the interaction U and the pairing field η. The remaining states with an odd average number of particles span two equivalent 4-dimensional subspaces (one for each spin channel) whose Hamiltonian projection reads

$$M_1 = \begin{pmatrix} -\frac{U}{2} & -t & -\eta & 0 \\ -t & -\frac{U}{2} & 0 & -\eta \\ -\eta & 0 & -\frac{U}{2} & t \\ 0 & -\eta & t & -\frac{U}{2} \end{pmatrix}. \tag{C10}$$

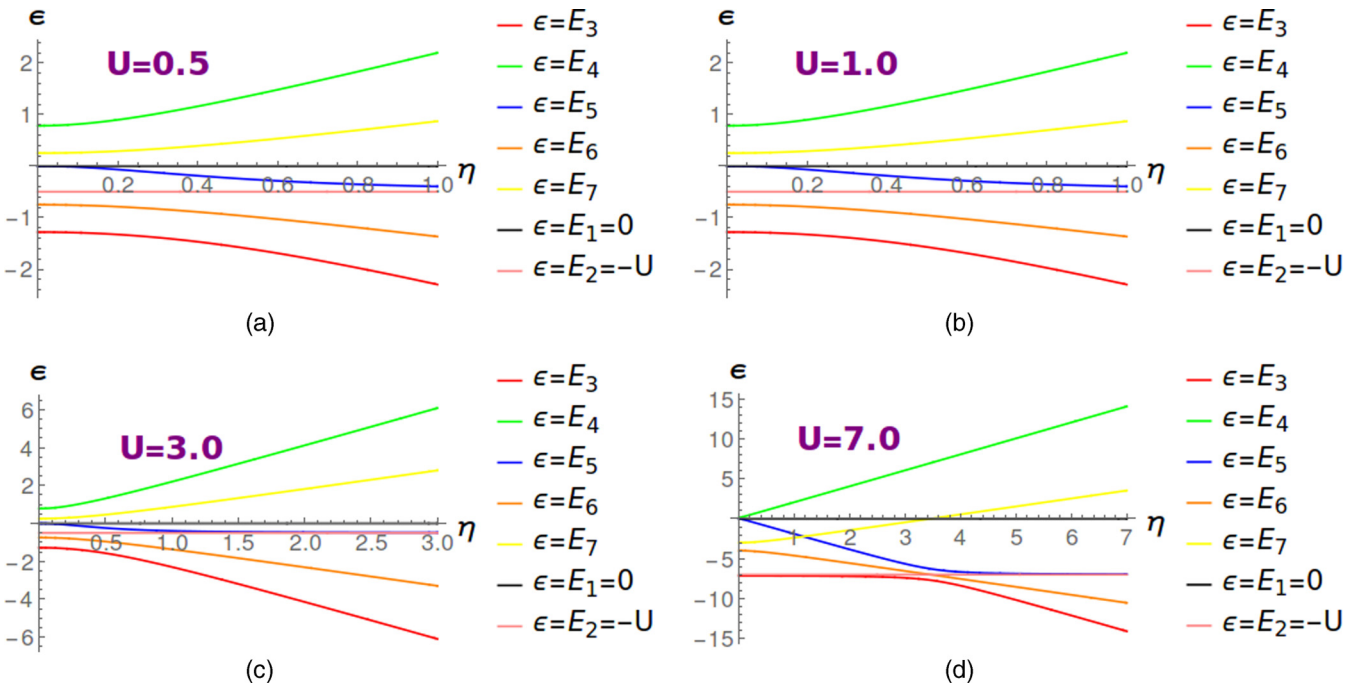

FIG. 12. Energy levels as a function of the pairing forcing field η for different values of U.

So we obtain the two eigenvalues E_6 and E_7 (each one four times degenerate) and the associated eigenvectors.

Figure 12 shows the seven eigenvalues as a function of η at different interaction values. Hence, it is possible to identify the state associated with E_3 to be the ground state of the system for any U and η values. This state lives in the subspace described by matrix M and can be written as follows:

$$|\mathrm{GS}\rangle = \alpha\left(\frac{|\uparrow,\downarrow\rangle - |\downarrow,\uparrow\rangle}{\sqrt{2}}\right) + \beta\left(\frac{|\uparrow\downarrow,0\rangle + |0,\uparrow\downarrow\rangle}{\sqrt{2}}\right) + \gamma\left(\frac{|0,0\rangle + |\uparrow\downarrow,\uparrow\downarrow\rangle}{\sqrt{2}}\right). \tag{C11}$$

Superconducting response at $T \neq 0$

The superconducting order parameter at finite temperature in the two-site model is readily computed as

$$\Delta = \frac{1}{2}\sum_i \frac{1}{Z}\mathrm{Tr}(e^{-\beta\hat{H}} c_{i\downarrow} c_{i\uparrow}) = \frac{1}{2}\frac{1}{Z}\sum_i \sum_{\tilde{n}\, n} e^{-\beta\epsilon_n} \langle\tilde{n}|c_{i_\downarrow}|n\rangle (\langle\tilde{n}|c^\dagger_{i\uparrow}|n\rangle)^*$$

$$= \frac{1}{Z}\{e^{-\beta E_6}(m_1 p_1 + m_2 p_2) + e^{-\beta E_7}(m_3 p_3 + m_4 p_4) + e^{-\beta E_3}(\beta_1\gamma_1) + e^{-\beta E_4}(\beta_2\gamma_2) + e^{-\beta E_5}(\beta_3\gamma_3)\}, \tag{C12}$$

where the coefficients m_i and p_i ($i = \{1,4\}$) are related to the eigenstates of M_1. Namely,

$$|E_6\rangle = l_{1(2)}|\uparrow,0\rangle + m_{1(2)}|0,\uparrow\rangle + n_{1(2)}|\uparrow,\uparrow\downarrow\rangle + p_{1(2)}|\uparrow\downarrow,\uparrow\rangle, \tag{C13}$$

$$|E_7\rangle = l_{3(4)}|\uparrow,0\rangle + m_{3(4)}|0,\uparrow\rangle + n_{3(4)}|\uparrow,\uparrow\downarrow\rangle + p_{3(4)}|\uparrow\downarrow,\uparrow\rangle, \tag{C14}$$

and the partition function is given by

$$Z = 3\, e^{\beta U} + 2 + e^{-\beta E_3} + e^{-\beta E_4} + e^{-\beta E_5} + 4e^{-\beta E_6} + 4e^{-\beta E_7}. \tag{C15}$$

Figure 7 shows the comparison between Eq. (C12) and the DMFT result for the superconducting order parameter.

[1] J. Bardeen, L. N. Cooper, and J. R. Schrieffer, Phys. Rev. **108**, 1175 (1957).
[2] R. Micnas, J. Ranninger, and S. Robaszkiewicz, Rev. Mod. Phys. **62**, 113 (1990).
[3] C. A. R. Sá de Melo, M. Randeria, and J. R. Engelbrecht, Phys. Rev. Lett. **71**, 3202 (1993).
[4] R. Haussmann, Z. Phys. B **91**, 291 (1993).
[5] F. Pistolesi and G. C. Strinati, Phys. Rev. B **53**, 15168 (1996).
[6] B. Kyung, S. Allen, and A.-M. S. Tremblay, Phys. Rev. B **64**, 075116 (2001).
[7] W. S. Bakr, J. I. Gillen, A. Peng, S. Fölling, and M. Greiner, Nature (London) **462**, 74 (2009).
[8] V. J. Emery and S. A. Kivelson, Nature (London) **374**, 434 (1995).
[9] Z. A. Xu, N. P. Ong, Y. Wang, T. Kakeshita, and S. Uchida, Nature (London) **406**, 486 (2000).

[10] Y. Wang, L. Li, M. J. Naughton, G. D. Gu, S. Uchida, and N. P. Ong, Phys. Rev. Lett. **95**, 247002 (2005).
[11] Y. Kosaka, T. Hanaguri, M. Azuma, M. Takano, J. C. Davis, and H. Takagi, Nat. Phys. **8**, 534 (2012).
[12] M. Norman, Nat. Phys. **10**, 357 (2014).
[13] T. Timusk and B. W. Statt, Rep. Prog. Phys. **62**, 61 (1999).
[14] J. C. Campuzano, M. R. Norman, and M. Randeria, *Physics of Superconductors*, Vol. II, edited by K. H. Bennemann and J. B. Ketterson (Springer, Berlin, 2004), pp. 167–273.
[15] E. Gull and A. J. Millis, Phys. Rev. B **86**, 241106 (2012).
[16] J. Merino and O. Gunnarsson, Phys. Rev. B **89**, 245130 (2014).
[17] O. Gunnarsson, T. Schäfer, J. P. F. LeBlanc, E. Gull, J. Merino, G. Sangiovanni, G. Rohringer, and A. Toschi, Phys. Rev. Lett. **114**, 236402 (2015).
[18] A. Toschi, M. Capone, and C. Castellani, Phys. Rev. B **72**, 235118 (2005).
[19] A. Georges, G. Kotliar, W. Krauth and M. J. Rozenberg, Rev. Mod. Phys. **68**, 13 (1996).
[20] W. Metzner and D. Vollhardt, Phys. Rev. Lett. **62**, 324 (1989).
[21] M. Keller, W. Metzner, and U. Schollwöck, Phys. Rev. Lett. **86**, 4612 (2001).
[22] A. Toschi, P. Barone, M. Capone, and C. Castellani, New J. Phys. **7**, 7 (2005).
[23] A. Garg, H. R. Krishnamurthy, and M. Randeria, Phys. Rev. B **72**, 024517 (2005).
[24] A. Amaricci and M. Capone, Phys. Rev. B **93**, 014508 (2016).
[25] C. Taranto, G. Sangiovanni, K. Held, M. Capone, A. Georges, and A. Toschi, Phys. Rev. B **85**, 085124 (2012).
[26] E. Gull, P. Werner, X. Wang, M. Troyer, and A. J. Millis, Europhys. Lett. **84**, 37009 (2008).
[27] H. J. A. Molegraaf *et al.*, Science **295**, 2239 (2002).
[28] A. F. Santander-Syro, R. P. S. M. Lobo, N. Bontemps, Z. Konstantinovic, Z. Li, and H. Raffy, Phys. Rev. Lett. **88**, 097005 (2002).
[29] A. F. Santander-Syro, R. P. S. M. Lobo, N. Bontemps, Z. Konstantinovic, Z. Z. Li, and H. Raffy, Europhys. Lett. **62**, 568 (2003).
[30] J. P. Carbotte and E. Schachinger, J. Low. Phys. **144**, 61 (2006).
[31] M. M. Qazilbash *et al.*, Nat. Phys. **5**, 647 (2009).
[32] L. Benfatto, S. Sharapov, and H. Beck, Eur. Phys. J. B **39**, 469 (2004).
[33] A. Toschi, M. Capone, M. Ortolani, P. Calvani, S. Lupi, and C. Castellani, Phys. Rev. Lett. **95**, 097002 (2005).
[34] L. Baldassarre *et al.*, Phys. Rev. B **77**, 113107 (2008).
[35] A. Toschi and M. Capone, Phys. Rev. B **77**, 014518 (2008).
[36] D. Nicoletti *et al.*, Phys. Rev. Lett. **105**, 077002 (2010).
[37] G. Deutscher, A. F. Santander-Syro, and N. Bontemps, Phys. Rev. B **72**, 092504 (2005).
[38] F. Carbone, A. B. Kuzmenko, H. J. A. Molegraaf, E. van Heumen, V. Lukovac, F. Marsiglio, D. van der Marel, K. Haule, G. Kotliar, H. Berger, S. Courjault, P. H. Kes, and M. Li, Phys. Rev. B **74**, 064510 (2006).
[39] M. Capone, M. Fabrizio, C. Castellani, and E. Tosatti, Science **296**, 2364 (2002).
[40] Y. Nomura, S. Sakai, M. Capone, and R. Arita, Sci. Adv. **1**, e1500568 (2015).
[41] G. Keller, K. Held, V. Eyert, D. Vollhardt, and V. I. Anisimov, Phys. Rev. B **70**, 205116 (2004).
[42] V. I. Anisimov, A. S. Belozerov, A. I. Poteryaev, and I. Leonov, Phys. Rev. B **86**, 035152 (2012).
[43] A. E. Antipov, I. S. Krivenko, V. I. Anisimov, A. I. Lichtenstein, and A. N. Rubtsov, Phys. Rev. B **86**, 155107 (2012).
[44] A. I. Lichtenstein, M. I. Katsnelson, and G. Kotliar, Phys. Rev. Lett. **87**, 067205 (2001).
[45] S. V. Vonsovsky, M. I. Katsnelson, and A. V. Trefilov, Phys. Met. Metallogr **76**, 247 (1993).
[46] A. Galler, C. Taranto, M. Wallerberger, M. Kaltak, G. Kresse, G. Sangiovanni, A. Toschi, and K. Held, Phys. Rev. B **92**, 205132 (2015).
[47] A. Toschi, R. Arita, P. Hansmann, G. Sangiovanni, and K. Held, Phys. Rev. B **86**, 064411 (2012).
[48] Z. P. Yin, K. Haule, and G. Kotliar, Nat. Phys. **7**, 294 (2011).
[49] D. Fausti, R. I. Tobey, N. Dean, S. Kaiser, A. Dienst, M. C. Hoffmann, S. Pyon, T. Takayama, H. Takagi, and A. Cavelleri, Science **331**, 189 (2012).
[50] C. Giannetti, M. Capone, D. Fausti, M. Fabrizio, F. Parmigiani, and D. Mihailovic, Adv. Phys. **65**, 58 (2016).
[51] R. Mankowsky, A. Subedi, M. Forst, S. O. Mariager, M. Chollet, H. T. Lemke, J. S. Robinson, J. M. Glownia, M. P. Minitti, A. Frano, M. Fechner, N. A. Spaldin, T. Loew, B. Keimer, A. Georges, and A. Cavalleri, Nature (London) **516**, 71 (2014).
[52] D. Fausti, F. Novelli, G. Giovannetti, A. Avella, F. Cilento, L. Patthey, M. Radovic, M. Capone, and F. Parmigiani, arXiv:1408.0888.
[53] M. Mitrano, A. Cantaluppi, D. Nicoletti, S. Kaiser, A. Perucchi, S. Lupi, P. Di Pietro, D. Pontiroli, M. Riccò, S. R. Clark, D. Jaksch, and A. Cavalleri, Nature (London) **530**, 461 (2016).
[54] T. Maier, M. Jarrell, T. Pruschke, and Matthias H. Hettler, Rev. Mod. Phys. **77**, 1027 (2005).